AlMidfa, K., Temeh, E. K., & Nix, A. R. (2000). Improved DOA estimation using polarisation diversity : simulations using a wideband propagation model. In International Symposium on Personal, Indoor and Mobile Radio Communications, 2000 (PIMRC 2000). (Vol. 1, pp. 539 - 543). Institute of Electrical and Electronics Engineers (IEEE). 10.1109/PIMRC.2000.881482

# Improved DOA Estimation using Polarisation Diversity: Simulations using a Wideband Propagation Model

Khalid AlMidfa, Eustace Tameh and Andrew Nix
University of Bristol, Centre for Communications Research
Merchant Venturers Building, Bristol BS8 1UB, UK
Tel: +44 (0)117 954 5203 Fax: +44 (0)117 954 5206
*e-mail*: k.almidfa@bristol.ac.uk

## ABSTRACT

This paper investigates the performance of a number of Direction-Of-Arrival (DOA) estimation algorithms in a wideband macrocellular channel using a dual-polarised antenna array. The signal data is obtained from a new spatial-temporal three-dimensional deterministic propagation model. The model was developed to meet the hierarchical network planning needs of third generation (3G) networks. Results show that a three-fold theoretical and two-fold practical improvement in DOA estimation accuracy can be achieved by exploiting information from a dual-polarised array.

## I. INTRODUCTION

The use of adaptive antennas at the basestation is likely to play an important role in emerging third generation (3G) mobile systems [1]. This is due to the antenna's ability to overcome many of the key problems associated with current mobile radio systems. Adaptive antenna benefits include a reduction in delay spread, interference and multipath fading, in addition to increased coverage, diversity gain and spectrum efficiency [2]. The use of dual-polarised antenna elements can provide additional degrees of freedom for the adaptive antenna system. This is considered by many to be an integral part of third generation antenna systems [3].

Previous work has shown that a number of DOA estimation algorithms can be used to estimate signal polarisation along with arrival angle [4]-[8]. More recently, several measurement campaigns studying spatio-temporal and polarisation effects using dual-polarised antenna arrays have been reported [4], [9]-[10]. Pedersen *et. al* [11] has suggested a radio channel model that includes the important effects of polarisation.

In this paper we show the results of applying DOA estimation algorithms on data obtained from a fully deterministic wideband propagation model. This model was developed at the University of Bristol to meet the planning needs of third generation wireless systems [12]-[13]. The DOA estimation algorithms considered here include Root-MUSIC, TLS-ESPRIT (Total Least Square Estimation of Signal Parameters via Rotational Invariance Techniques) and Unitary ESPRIT.

The wideband propagation model is described in Section II. In Section III the signal model used in these simulations is formulated and described. The simulation set-up is covered in section IV with results discussed in Section V. The paper ends with a set of conclusions based on the results shown.

0-7803-6465-5/00 $10.00 © 2000 IEEE

## II. WIDEBAND PROPAGATION MODEL

One of the main features of UMTS is the support of mixed-cell (or hierarchical cell) structures. However, propagation characteristics vary significantly for different environments – from indoor environments to urban and open rural areas. As such, in order to provide accurate information for planning third generation (3G) networks, propagation models need to be able to accommodate propagation in mixed-cell scenarios, *i.e.* they need to integrate macro-, micro-, and picocellular propagation characteristics. With the proposed use of adaptive antenna technology to improve system performance in 3G systems, there is a strong requirement for time dispersion and spatial information (arrival angles at the BS and MS). A fully 3-D wideband propagation model has been developed that predicts temporal and spatial dispersion in mixed (macro- and microcellular) deterministic environments. The model also provides coverage and fading information [12].

### *Model Description*

The model uses a variable resolution Digital Terrain Map (DTM) to model irregular terrain up to 10km × 10km in size, a 10m resolution raster building database for built-up areas, as well as foliage and ground-cover databases in the prediction area [12].

Each illuminated terrain pixel and building wall contributes a unique propagation path between the BS and MS. The power contributed by each scattering surface is obtained from the radar equation:

$$P_r = \frac{P_t G_t(\theta,\phi) G_r(\theta,\phi) \lambda^2 \sigma^{ij}}{(4\pi)^3 R_t^2 R_r^2} L \qquad (1)$$

where, $\sigma^{ij}$ is the polarimetric bistatic radar cross section (RCS) of the surface, the superscripts $ij$ refer to two orthogonal polarisation states (*e.g.* vertical and horizontal), $P_t$ is the total transmitted power, $G_t(\theta,\phi)$ and $G_r(\theta,\phi)$ are the BS and MS antenna gains in the direction $(\theta,\phi)$, respectively, $R_t$ and $R_r$ are the distances from the pixel to the BS and MS, respectively, and $L$ is the total diffraction and foliage loss in the two path profiles.

The polarimetric bistatic RCS is obtained using the Kirchhoff and Small Perturbation models [14]. A

polarimetric scattering cross-section matrix $[\sigma]$ is then calculated as:

$$[\sigma]=\begin{bmatrix}\sigma^{ii} & \sigma^{ij}\\ \sigma^{ji} & \sigma^{jj}\end{bmatrix} \quad (2)$$

where the first superscript denotes the transmit polarisation and the second superscript the receive polarisation. Since the polarisation of any plane wave can be described in terms of two orthogonal, linearly polarised components, the matrix $[\sigma]$ contains all the polarisation properties of the target. The scattered power for any given combination of transmit and receive polarisation states can then be calculated.

The use of a novel variable terrain resolution technique has produced a significant speed-up in the model execution time for large areas [13]. Free space propagation is assumed in the direct path between the BS and MS. In addition to the free space loss, the model adds a diffraction loss for a user-specified number of diffraction edges, losses due to the presence of foliage in the path and to inadequate Fresnel zone clearance.

The model predicts signal strength, time dispersion (complex impulse response and delay spread), fast fading (Rician K factor) as well as arrival angles for all rays at the BS and MS. Predictions are made for single MS (points), multiple MS points (random locations or locations along a specified route), as well as for specified areas (grids).

Figure 1 shows a sample output of the model for a specified BS and MS location. It shows the 10 strongest ray paths from the BS to the MS. The model has been validated through measurements in both urban and rural environments with good agreement observed between the predictions and measurements [12]-[13] (RMS error ≈ 6-8dB). The measurements have further emphasised the importance of considering foliage attenuation in the propagation model, with errors of up to 18dB observed when foliage effects are ignored in the prediction. Figure 2 shows a signal strength profile for a route in the city centre of Bristol, comparing the measured and predicted signal levels.

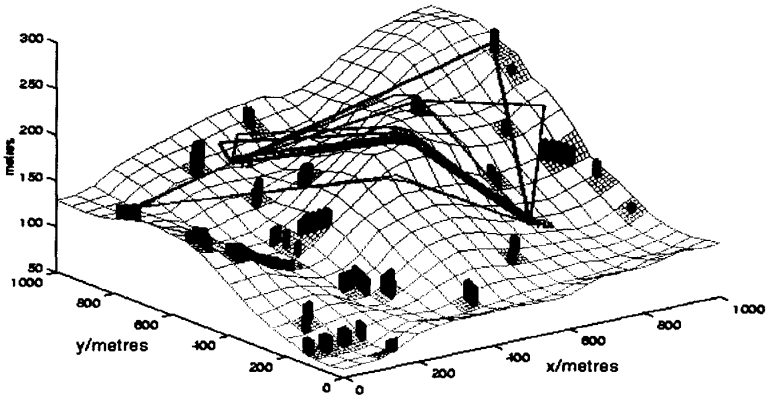


*Figure 1: Variable resolution DTM with 10 strongest rays from TX (BS) to RX (MS).*

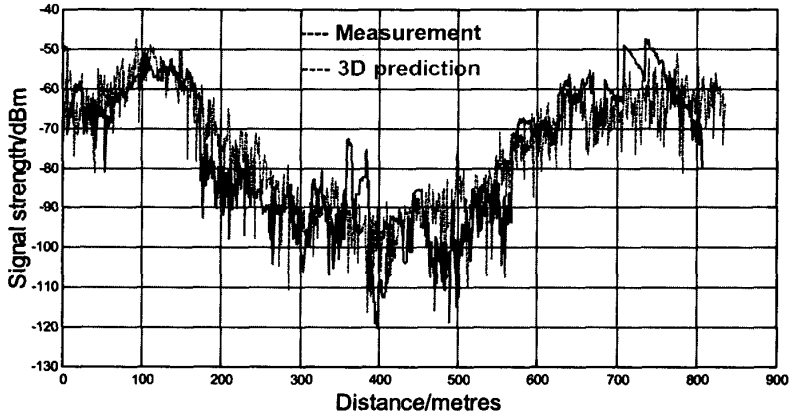


*Figure 2: Measured and predicted signal strength profiles.*

## III. SIGNAL MODEL WITH POLARISATION INFORMATION

The signal model developed in this section assumes that a single location parameter is to be used per signal, *i.e.* the azimuth angle (DOA) of the dominant multipath. Also, the signal sources are assumed to be in the far-field of the antenna array so that the signal wavefronts are effectively planar over the array.

Consider an antenna array which consists of $N$ dual-polarised sensors on which plane waves from $M$ ($M < N$) narrow-band sources impinge from directions $\theta_1, \ldots, \theta_M$. Let $y(t)$ be the complex vector received by the array:

$$y(t) = As(t) + w(t) \tag{3}$$

where $s(t)$ is the signal vector, $w(t)$ is the additive noise vector, which is assumed to be modelled as a temporally white and zero-mean complex Gaussian process. $A$ is referred to as the *array response* or *array steering vector* and is defined as [6]:

$$A_{nm} = \left[\cos(\gamma_m) + \sin(\gamma_m) e^{j\eta_n}\right] \cdot e^{-j\omega_0 \tau_{nm}} \tag{4}$$

where $\gamma_m$ is the polarisation angle of the $m$-th source, $\eta_n$ is the polarisation angle of the $n$-th sensor and $\tau_{nm}$ is the delay associated with the signal propagation time from the $m$-th source to the $n$-th sensor and is given by:

$$\tau_{nm} = -\frac{1}{c}\left[\bar{x}_n \sin\theta_m + \bar{y}_n \cos\theta_m\right] \tag{5}$$

where $c$ is the propagation velocity and $(\bar{x}_n, \bar{y}_n)$ are the co-ordinates of the $n$-th sensor.

Now, the covariance matrix of the received signal data can be defined as:

$$R = E[y(t) y^H(t)] \tag{6}$$

where $E[\cdot]$ and $^H$ denote the expectation operator and the conjugate transpose, respectively. From our assumptions $R$ can also be represented as follows (recognising also that $s(t)$ and $w(t)$ are statistically independent):

$$R = ASA^H + \sigma_w^2 I \tag{7}$$

where $S$ represents the signals' covariance matrix ($S = E[s(t)s^H(t)]$), $\sigma^2$ is the noise power at each antenna and $I$ denotes an $N \times N$ identity matrix.

The subspace methods used in this paper utilise the special eigenstructure of the covariance matrix $R$ as explained in [5,15].

## IV. SIMULATION SETUP

The wideband propagation model described in section II is used to generate prediction data for 20 different MS location points with fixed BS location. This is repeated for the four combinations of polarisation as shown in Equation (2). Therefore, for each point all parameters used in the propagation model are fixed except for the polarisation. This can be considered as diversity reception where, for each polarisation of the transmitting MS, the signal is received at the BS by an 8-element dual polarised antenna array.

The resulting prediction data is then used in the simulations where the stationary MS transmits a WCDMA signal received by the BS. The WCDMA signal was generated following the ETSI UMTS Terrestrial Radio Access (UTRAN) RTT proposal to ITU-R [16]. Table 1 summarises the values of some of the parameters employed in the simulations.

| Parameter | Value |
|---|---|
| Frequency (MHz) | 2000 |
| No. of Antenna Elements ($N$) | 8 |
| Inter-Element Spacing ($d$) | $\lambda/2$ |
| WCDMA chip rate (k chips/sec) | 3840 |
| WCDMA data rate (kbps) | 16 |
| Signal-to-Noise Ratio (dB) | 20 |

*Table 1: Parameters used in the simulations.*

The prediction data for each ray used in the simulations includes: time of arrival (TOA), power, phase, azimuth angle at the BS (DOA) and the polarisation of the transmitting and receiving antennas. Power windows are applied to filter out weak rays and rays are put into time bins according to their TOAs (based on the WCDMA chip rate). Note that rays with DOA outside the angular aperture of the receiving array, which is assumed ±60° from array boresight, are also filtered.

The antenna array response is then generated using the DOAs and the polarisations of the MS and BS, as shown in Equation (4). The eigenvalue decomposition of the covariance matrix, $R$, is then derived and used in the DOA estimation algorithms.

## V. SIMULATION RESULTS

In this study Selection (Switched) Diversity has been chosen as the combining method at the BS. The aim of the algorithm is to switch to the polarisation that enables a more accurate DOA estimation to be performed. However, there is no published work discussing the switching criterion that should be used. Two different criteria are proposed in this paper: these are the Total Power Level (TPL) and the multipath Peak-to-Sidelobe Level (PSL). Results for these criteria are then compared to the theoretically ideal case, where both branches are processed and the lowest DOA error is selected.

In the first criteria, TPL, the diversity branch receiving the highest power level is chosen, whereas in the second criteria, PSL, the branch with the higher peak-to-multipath-sidelobe level is chosen (*i.e.* the branch with a more deterministic signal).

Figure 3 shows the Root-MUSIC DOA estimation error for the azimuth direction (relative to the strongest multipath) for both diversity branches when the MS is horizontally polarised. The mean value of the DOA estimation error is 1.25° and 2.09° when the BS is horizontally and vertically polarised respectively.

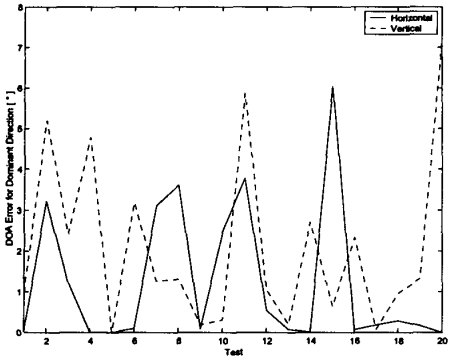


*Figure 3: DOA estimation error of the dominant direction estimated by Root-MUSIC for the two diversity branches.*

Figure 4 shows the results when ideal diversity switching is now applied between the two branches, i.e. the minimum DOA error is always chosen. The mean DOA estimation error drops from a worst case 2.09° to just 0.66° (a three-fold reduction). Using the practical switching criteria, the mean DOA estimation error is calculated at 1.84° (TPL) and 1.08° (PSL) respectively. For the practical PSL approach, almost a two-fold reduction in the DOA error is achieved. These figures indicate that the PSL method is better suited to the task of diversity switching when the Root MUSIC algorithm is used. Table 2 summarises the findings of the above simulations for Root MUSIC and also gives the results for a vertically polarised MS, which agree well with the earlier results.

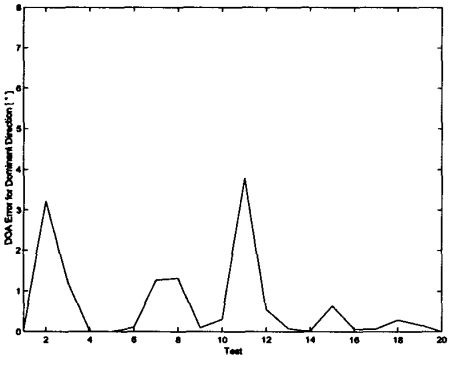


*Figure 4: Minimum DOA estimation error between the two diversity branches of the dominant direction estimated using Root-MUSIC.*

| MS (Tx) | BS (Rx) | Mean(Peak) | Switching Diversity Method: Ideal | Total Power Level | Peak-to-Sidelobe Level |
|---|---|---|---|---|---|
| H | H | 1.25(6.04) | 0.66 | 1.84 | 1.08 |
| | V | 2.09(7.16) | | | |
| V | H | 1.36(3.83) | 0.73 | 2.04 | 1.32 |
| | V | 2.04(11.40) | | | |

*Table 2: Mean DOA estimation error, in degrees, of dominant direction estimated by Root MUSIC.*

Table 3 shows the mean DOA estimation error obtained using TLS-ESPRIT. Here diversity switching based on the peak-to-sidelobe level still produces the better performance when compared to power level based switching.

| MS (Tx) | BS (Rx) | Mean(Peak) | Switching Diversity Method: Ideal | Total Power Level | Peak-to-Sidelobe Level |
|---|---|---|---|---|---|
| H | H | 1.74(10.07) | 0.80 | 2.42 | 1.78 |
| | V | 2.06(7.12) | | | |
| V | H | 1.36(3.86) | 0.71 | 2.69 | 2.13 |
| | V | 2.69(11.97) | | | |

*Table 3: Mean DOA Estimation Error, in Degrees, of Dominant Direction Estimated by TLS ESPRIT.*

Table 4 shows the mean DOA estimation error obtained using the Unitary-ESPRIT algorithm. Once again, the peak-to-sidelobe level diversity switching approach produces the better performance.

| MS (Tx) | BS (Rx) | Mean(Peak) | Switching Diversity Method: Ideal | Total Power Level | Peak-to-Sidelobe Level |
|---|---|---|---|---|---|
| H | H | 1.49(5.74) | 0.50 | 1.86 | 1.16 |
| | V | 1.34(4.07) | | | |
| V | H | 1.36(4.38) | 0.81 | 2.51 | 1.64 |
| | V | 2.69(8.57) | | | |

*Table 4: Mean DOA estimation error, in degrees, of dominant direction estimated by Unitary ESPRIT.*

From the tables above it can be seen that in some specific cases the results obtained for horizontally polarised array data are slightly better than those achieved using the peak-to-sidelobe diversity approach. This implies that the current criteria are sub-optimal. The results shown for an ideal dual-polarised antenna selection algorithm demonstrate that switching can lower the DOA estimation error in all the cases and for all the DOA estimation algorithms considered here.

## VI. CONCLUSIONS

In this paper the performance of Root-MUSIC, TLS-ESPRIT and Unitary-ESPRIT have been investigated using a dual-polarised antenna array. This was performed using data obtained from a wideband propagation model that predicts temporal and spatial dispersion in mixed (macro- and micro-) cellular environments. DOA estimation algorithms have been applied at the BS to find the DOA of the signal transmitted by a single static MS as a function of polarisation.

Results indicate that the mean DOA estimation error can be reduced by a factor of three using ideal diversity switching to exploit the polarisation information at the BS.

Two practical switching metrics have been considered in this paper, namely total power and multipath peak-to-sidelobe level. Results for both criteria have been shown to offer improvements (approximately halving the mean DOA error), but both fall short of the ideal switching result. Based on the research performed to date, switching based on the peak-to-sidelobe level appears to offer a better result.

In conclusion, further work is required to determine a more appropriate switching criterion to fully exploit the theoretical benefits of polarisation diversity in the area of DOA estimation.

***Acknowledgements***

K. AlMidfa would like to thank Emirates Telecommunications Corporation-ETISALAT for sponsoring his PhD. studies. The authors are also grateful for the help and support of their colleagues at the Centre for Communications Research, most notably Dr Mark Beach, for his useful comments and insights in the area of polarisation diversity.

## REFERENCES

[1] Sheikh, K., Gesbert, D., Gore, D. and Paulraj, A., "Smart Antennas for Broadband Wireless Access Networks", IEEE Comm. Mag., Vol. 37, No. 11, Nov. 1999, pp.100-105.

[2] Godara, L.C., "Application of Antenna Arrays to Mobile Communications, Part I: Performance Improvement, Feasibility, and System Considerations", Proc. of IEEE, Vol. 85, No. 7, Jul. 1997, pp. 1031-1060.

[3] Nilsson, M., Lindmark, B, Ahlberg, M., Larsson, M. and Beckman, C., "Measurements of the Spatio-Temporal Polarisation Characteristics of a Radio Channel at 1800MHz", VTC '99, pp. 386-391, Houston, TX, May 1999.

[4] Schmidt, R., "A Signal Subspace Approach to Multiple Emitter Location and Spectral Estimation", PhD. Thesis, Stanford University, Stanford, CA, Nov. 1981.

[5] Ferrara, E.R. and Parks, T.M., "Direction Finding with an Array of Antenna Having Diverse Polarisations", IEEE Trans. A&P, Vol. AP-31, No. 2, Mar. 1983, pp. 231-236.

[6] Weiss, A.J. and Friedlander, B., "Performance Analysis of Diversely Polarised Antenna Arrays", IEEE Trans. SP, Vol. 39, No. 7, Jul. 1991, pp. 1589-1603.

[7] Li, J. and Compton, T. Jr., "Angle and Polarisation Estimation Using ESPRIT with a Polarisation Sensitive Array", IEEE Trans. A&P, Vol. 39, No. 9, Sep. 1991, pp. 1376-1383.

[8] Swindlehurst, A. and Viberg, M., "Subspace Fitting with Diversely Polarised Antenna Arrays", IEEE Trans. A&P, Vol. 41, No. 12, Dec. 1993, pp. 1687-1694.

[9] Bengtsson, M., Astély, D. and Ottersten, B., "Measurements of Spatial Characteristics and Polarisation with Dual Polarised Antenna Array", VTC '99, pp. 366-370, Houston, TX, May 1999.

[10] Lindmark, B. and Nilsson, M., "Polarisation Diversity Gain and Base Station Antenna Characteristics", VTC '99, pp. 590-595, Houston, TX, May 1999.

[11] Pedersen, K.I., Mogensen, P.E. and Fleury, B.H., "Dual-Polarised Model of Outdoor Propagation Environments for Adaptive Antennas", VTC '99, pp. 990-995, Houston, TX, May 1999.

[12] Tameh, E.K., Nix, A.R. and Beach, M.A., "A 3-D integrated macro and microcellular propagation model, based on the use of photogrammetric terrain and building data", VTC '97, pp. 1957-1961, Phoenix, Arizona, May 1997.

[13] Tameh, E.K. and Nix, A.R., "The Use of Measurement Data to Analyse the Performance of Rooftop Diffraction and Foliage Loss Algorithms in a 3-D Integrated Urban/Rural Propagation Model", VTC '98, pp. 303-307, Ottawa, Canada, May 1998.

[14] Lebherz, M., Wiesbeck, W. and Krank, W., "A versatile Wave Propagation Model for the VHF/UHF Range Considering Three-Dimensional Terrain", IEEE Trans. Comm., Vol. 40, Oct. 1992, pp 1121-31.

[15] AlMidfa, K., Tsoulos and Nix, A., "Performance Evaluation of Direction-of-Arrival (DOA) Estimation Algorithms for Mobile Communication Systems", VTC2000-Spring, pp. 1055-1059, Tokyo, Japan, May 2000.

[16] ETSI SMG2: 'Evaluation Report for ETSI UMTS Terrestrial Radio Access (UTRA) ITU-R RTT Candidate", 1999.